

# Comparison of Monte-Carlo Modeling and Experimental Results of UV-emission from Engine Exhaust Plume Interacting with Upper Atmosphere

Alexander I. Erofeev<sup>†</sup>, Oscar G. Friedlander<sup>†</sup>, George F. Karabadzhak\*,  
Yurii A. Plastinin\*,

<sup>†</sup>*Central Aerohydrodynamic Institute (TsAGI), Zhukovsky, 140180, Moscow Region, Russia*

\**Central Institute for Machine Building (TsNIMASH), Korolev, 141070, Moscow Region, Russia*

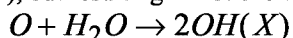
**Abstract.** Approximate method for Monte-Carlo modeling of interaction of high-altitude engine exhaust plume with atmosphere has been developed. The method was applied for analysis of recent experimental data on Russian spacecraft Soyuz plume glow. In particular, sensitivity of computed glow radiation to the choice of elastic collision cross-section of atmospheric oxygen with plume molecules and its reaction cross-section with water molecules in the plume is analyzed. Conclusions are made about these cross-sections values.

## INTRODUCTION

A set of experiments dedicated to measurement of Russian spacecraft (SC) Soyuz and Progress plume glow in the region 270-340 nm at altitudes of 360-400 km was accomplished recently on board of Russian Space Station Mir [1-4]. In this experiments radiometric data on the intensity and spatial distribution of the radiation in the SC motor plumes were acquired. A hypothesis was put forward that radiation is a product of the hypervelocity reaction between water molecules available in plume with atmospheric oxygen atoms



The UV glow was observed in the region extended over some kilometers from the SC motor. Several papers have been published by now where this glow was modeled by DSMC method [5-7]. Results of the modeling overpredict the experimental data on one or two orders of magnitude, depending on the model parameters. Conclusion was made that main source of this discrepancy might be not appropriately chosen model parameters, such as elastic and reaction (1) cross-sections. No direct measurements or accurate computation of the cross-section values in the range of collision energies relevant to the experiment are known so far. So, for modeling of these cross-sections authors used VHS and TCE models correspondingly and the model parameters were derived by extrapolating of the parameters defined at low energetic collision to the high energetic collision case. VHS model parameters were used as those obtained from the viscosity measurements. Whereas, parameters of TCE model were derived from measured rate constant of the reaction (1), but resulting in not excited products



Such approach was not completely satisfying from the standpoint of the comparison with experimental data. Therefore, necessity arises to analyze the glow phenomena in more detail and revise more accurate collision cross-section values basing on the newly obtained experimental data. This analysis requires a vast amount of parametric computation and can not be effectively accomplished basing on the time consuming full scale DSMC. As an alternative, a simplified physically transparent model of the glow was developed for the data analysis. In this model averaged elastic cross-section values are used to compute the flow-field and overlay method is employed for radiation computation. In comparison with full DSMC the simplified computation requires much less time resulting in the same outputs. First attempts to apply this model to analysis of the experimental data fully justified the approach.

## Report Documentation Page

|  |  |  |
|--|--|--|
| <b>Report Date</b><br>09JUL2000  | <b>Report Type</b><br>N/A                          | <b>Dates Covered (from... to)</b><br>-       |
| <b>Title and Subtitle</b><br>Comparison of Monte-Carlo Modeling and Experimental Results of UV-emission from Engine Exhaust Plume Interacting with Upper Atmosphere                                |  | <b>Contract Number</b>                       |
|  |  | <b>Grant Number</b>                          |
|  |  | <b>Program Element Number</b>                |
| <b>Author(s)</b>   | <b>Project Number</b>                              |  |
|  | <b>Task Number</b>                                 |  |
|  | <b>Work Unit Number</b>                            |  |
| <b>Performing Organization Name(s) and Address(es)</b><br>Central Aerohydrodynamic Institute (TsAGI), Zhukovsky, 140180, Moscow Region, Russia   |  | <b>Performing Organization Report Number</b> |
| <b>Sponsoring/Monitoring Agency Name(s) and Address(es)</b><br>AOARD Unit 45002 APO AP 96337-5002  |  | <b>Sponsor/Monitor's Acronym(s)</b>          |
|  |  | <b>Sponsor/Monitor's Report Number(s)</b>    |
| <b>Distribution/Availability Statement</b><br>Approved for public release, distribution unlimited  |  |  |
| <b>Supplementary Notes</b><br>Papers from Rarefied Gas Dynamics (RGD) 22nd International Symposium held in Sydney, Australia on 9-14 July 2000. See also ADM001341 for whole conference on cd-rom. |  |  |
| <b>Abstract</b>  |  |  |
| <b>Subject Terms</b>   |  |  |
| <b>Report Classification</b><br>unclassified   | <b>Classification of this page</b><br>unclassified |  |
| <b>Classification of Abstract</b><br>unclassified  | <b>Limitation of Abstract</b><br>UU                |  |
| <b>Number of Pages</b><br>7  |  |  |

## 2. PHYSICAL AND COMPUTATIONAL MODEL

### 2.1. Input data for model statement.

The mathematical model is intended for the analysis of concrete experimental data. Therefore standard conditions of realization of experiment are presented below. The common scheme of observations is shown on Fig. 1. Two schemes of observation were applied: a) observation « in a tail », at a small viewing angle  $\beta$ , and observation from the side at tangent angle  $\beta \approx 90^\circ$ . In both schemes the pitch angle  $\alpha$  did not exceed  $17^\circ$ .

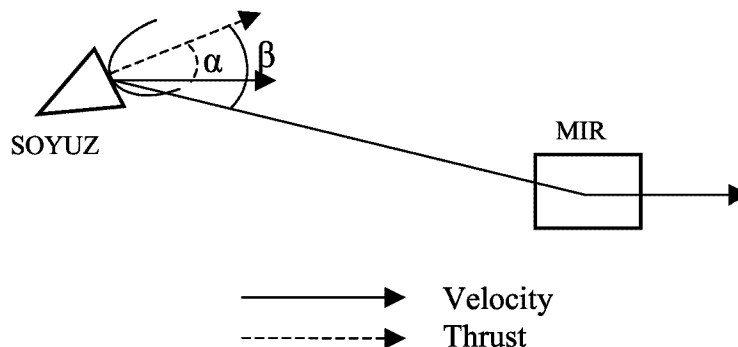


FIGURE 1. Scheme of space experiment.

The MIR-SOYUZ range varies from 11 km up to 25 km. For numerical simulation the standard values of parameters of a trajectory and atmosphere were selected:

$$H=360-400 \text{ km}, V=7.35 \text{ km/s}, n_a=1.34 \cdot 10^{14} \text{ m}^{-3}, T=886 \text{ K},$$

$$X(O)=0.909, X(He)=0.0517, X(N_2)=0.0393.$$

Here  $X(M)$  is a mole fraction of M gas component.

As the initial data for calculation of rarefied flow of gases the data obtained at solution of continuum equations (up to distance about 20 meters from the nozzle exit section) were used. The following values of parameters were adopted on plume axis at  $x=20.18m$ : density  $n=0.331 \cdot 10^{20} \text{ m}^{-3}$ , gas velocity (in a nozzle coordinate system)  $u=3335 \text{ m/s}$  and temperature  $T=37.52K$ .

It was supposed, that the signal of UF-imager mainly was defined by the contribution of an emission  $OH(A \rightarrow X)$ . The characteristics of reaction (1) are those: threshold energy  $E_{th}=4.83eV$ , lifetime of excited molecules  $\tau=10^{-9} \text{ s}$  and average energy of quantum  $h\nu=6.43 \cdot 10^{-19} \text{ J}$ .

### 2.2. Mathematical model

#### 2.2.1. Simple physical model.

The input data and notion about emission source allow to present the simplified physical model. Let's consider plume in a spacecraft coordinate system, with the nozzle as an origin. It is well known, that density in plume is proportional to  $(x/x_*)^{-2}$ , where  $x$  - distance up to a nozzle. This dependence enables to estimate the distance, on which numerical density in plume is compared to numerical density of gas of a nonperturbed atmosphere:  $L_1 \approx 10 \text{ km}$ . Such estimate displays the weak influence of an atmosphere on a plume field at a distance of about 1 km. On distances comparable with  $L_1$ , it is necessary to take into account the interaction of a plume and atmosphere.

Temperature of a plume is so low, that it is possible to neglect by thermal velocity of plume molecules. The threshold of process (1) is high. Therefore it happens, in main, owing to existence of oxygen atoms thermal velocity. If the oxygen atom has collision with a plume molecule, then, first, it removes from area, close to plume axis, and,

secondly, its velocity decreases. Therefore the energy of relative motion of oxygen atoms and molecules of water becomes lower energy of a threshold. Therefore at  $x < L_1$  it is admitted to consider following model of gas flow. The creation of a plume at  $x \ll L_1$  happens irrespectively to interaction with an atmosphere. The atoms of oxygen scattered on plume molecules. As the thermal velocity of oxygen atoms is much less than their average velocity, it is possible to accept the collision cross section  $\sigma_e$  to be constant in the flow. The generation of  $OH(A)$  results from  $O + H_2O$  collision according to probability of reaction (1).

### 2.2.2. Mathematical model.

The inelastic collisions frequency of water molecules with oxygen atoms which leads to emission is equal

$$W(\bar{x}) = \iint f_o(\bar{\xi}_o) f_1(\bar{\xi}_1) g\sigma_r(E) d\bar{\xi}_o d\bar{\xi}_1, E > E_{th}, \quad (2)$$

Here  $f_o, f_1$  are the velocity distribution functions of oxygen atoms and water molecules,  $\sigma_r(E)$  - inelastic collision cross section. In accordance to 2.2.1. these functions are the solutions of simplified Boltzmann equations:

$$\xi_k \frac{\partial f_i}{\partial x_k} = \sum_j J(f_i, f_j) \quad (3)$$

$$\xi_k \frac{\partial f_{oo}}{\partial x_k} = -f_{oo} \sum_i \int f_i g \sigma_i(\bar{\xi}_o, \bar{\xi}_i) d\bar{\xi}_i \approx -f_{oo} \left| \bar{\xi}_o - \bar{u} \right| \sigma_e n_{pl} \quad (4)$$

Here  $f_{oo}$  is the distribution function of oxygen atoms which move without collision with plume molecules,  $\sigma_e$  - effective elastic cross-section, and it was taken into account, that the change of relative concentrations of components in plume may be neglected. The equation (3) was solved by the DSMC method and linear equation (4) by the usual Monte-Carlo method. The solution of Eq.(3) have shown that the density of plume has the similarity.

### 2.2.3. Collision cross-section adopted values.

*Elastic cross-section.* The data on intermolecular potentials of oxygen atoms and plume molecules [8-10] are sparse. The most of data were obtained in experiments with scattering beam [8] for all components of a jet excepting  $H_2O$ . Let us compare the values of transport collision cross-section  $Q$  for  $O - N_2$  collision, calculated with the data of [8,10]. At average velocity of oxygen atoms these values are  $7.42 \cdot 10^{-20} m^2$  and  $7.96 \cdot 10^{-20} m^2$  accordingly. The estimate uses the Born-Mayer exponential repulsive potential. The cross-sections calculated with the help of Lennard-Jones potential are approximately twice more. The similar results may be obtained for the  $O - CO$  and  $O - CO_2$  collision cross-section. These estimates lead to parametric investigation at cross-section value range  $7.5 \cdot 10^{-20} m^2 \leq \sigma_e \leq 20 \cdot 10^{-20} m^2$ . Nevertheless authors suppose by more natural in the considered problem to use the cross-section values obtained in beam experiments.

*Inelastic cross-section.* The data on the process, interesting for us, practically miss. The collision model was used conventional for simulation of inelastic processes [11], though this form may be inadequate to the true process:

$$\sigma_r = \sigma_{0i} (E - E_{th,i})^{n_i} E^{-1}, E > E_{th,i} \quad (5)$$

Thus two sets of parameters values were used:  $n_1 = 0.5$ ,  $E_{th,1} = 4.83 eV$ ,  $\sigma_{01} = 1.15 \cdot 10^{-20} m^2 (eV)^{1/2}$ ;  $n_1 = 1.8$ ,  $E_{th,1} = 4.79 eV$ ,  $\sigma_{01} = 3.1 \cdot 10^{-20} m^2 (eV)^{-0.8}$ . The relation (5) closes a statement of mathematical model of processes (2), (3), (4), which leads to emission. This model enters splitting processes and allows to calculate scattering and inelastic collisions of oxygen atoms after the parameters of a plume are defined.

### 2.2.4. Analytical model.

Interaction of oxygen atoms with plume molecules (see Eq. (4)) in case of a cylindrical symmetry of may be described especially simply on axis. In this case it is possible approximately to split the description of processes leading to emission. Namely, to divide the process of elastic scattering of oxygen atoms and their inelastic

interaction with molecules of water. Let's assume, that  $f_{00}(x, \vec{\xi}) = n(x) \cdot f_{00,\infty}(\vec{\xi})$ . Integrating Eq.(4), substituting outcome in Eq.(2) and using a smallness of  $S_\infty^{-1}$ , we can receive:

$$W(x, r=0) = (\sigma_{r,eff} / \sigma_e) X(H_2O) X_\infty(O) n_a V \cdot x_*^{-1} K n_{pl,0} \cdot y^2 \exp(-y) \quad (6)$$

$$y = K n_{pl,0}^{-1} (x_* / x), \quad K n_{pl,0}^{-1} = (V + u) \cdot V^{-1} \sigma_e A \cdot n_{pl,0} \cdot x_*,$$

$$\sigma_{r,eff} = (X_\infty(O) \cdot n_a)^{-1} (V + u)^{-1} \int \sigma_r(E) g \cdot f_{00}(\infty) d\vec{\xi} \quad (7)$$

So simple computational model allows to make the following conclusions. The maximum value of inelastic collision frequency is reached at  $y = 2$ , i.e. at point  $x_{\max}$ , distance from which to nozzle is proportional  $\sigma_e$ . Maximum value  $W_{\max}$  is in inverse proportion to  $\sigma_e$ . If we observe the emission from infinitely large distance along a centerline the radiance will be peer

$$W_x = \frac{h\nu}{4\pi} \int_0^\infty W(x) dx = \frac{h\nu}{4\pi} X_{pl}(H_2O) \cdot X_\infty(O) \cdot n_a \cdot V \frac{\sigma_{r,eff}}{\sigma_e} \quad (8)$$

It is seen that the radiance is in inverse proportion to  $\sigma_e$ .

### 2.3. The model defects assessment.

#### 2.3.1. Error from the limitation of a computational area.

For the numerical modeling of the process (4) the conditions of a undisturbed flow are put on final distance from a nozzle  $L_{\max}$ . In this case in expression (8) there is a factor  $k_\infty$ :  $k_\infty = \exp(K n_{pl,0}^{-1} (x_* / L_{\max}))$ . The value of this coefficient at  $x_* = 19.18m$ ,  $L_{\max} = 15km$ ,  $\sigma_e = 15 \cdot 10^{-20} m^2$  is equal to 1.183. Thus, the limitation of an axial size of computational area by 15 km reduces the outcome near to an axis up to 18 %.

#### 2.3.2. Error caused by neglecting of plume molecule scattering.

Consider the process of plume molecule scatter at large distance from a nozzle in the same way, as the oxygen atoms scattering. It is easy to receive a following set of equations for the plume numerical density on an axis of a plume:

$$\frac{u}{x^2} \frac{\partial}{\partial x} (x^2 n_{pl}) = -n_{pl} n_a (V + u) \sigma_e, \quad V \frac{\partial}{\partial x} n_o = n_{pl} n_a (V + u) \sigma_e \quad (9)$$

The solution of equations (9) by the method of matched asymptotic expansions on the small parameter,  $(\varepsilon K n_{pl,0}^{-1})$ ,  $\varepsilon = (V + u) u^{-1} x_* \sigma_{e,a} n_a$ , we shall receive in main approximation:  $W_1 / W_2 = \exp(-\varepsilon x)$ . Here  $W_1$  - the value of radiance on axes appropriate to model, in which it is taken into account the plume scatter,  $W_2$  - the value appropriate to model without the scatter account. The ratio  $W_{x1} / W_{x2}$  under the observation from distance of 15 km is equal 0.877 and 0.785 for  $\sigma_{e,a} = 10 \cdot 10^{-20} m^2$  and  $15 \cdot 10^{-20} m^2$  accordingly. Thus, the neglecting by the plume scattering leads to an error about 20 %. Let's remark also, that the errors of models caused by limitation of computational area and neglecting by the plume scattering have different signs and partially cancel each other.

## SIMULATION RESULTS.

### 3.1. Models comparison.

The equations (2)-(5) of mathematical model, were solved by a Monte-Carlo method. The results obtained with the help of this model (curve 1) are compared in a Fig. 2a to the analytical profile  $W(x,0)$  (see eq. (6) – curve 2) and

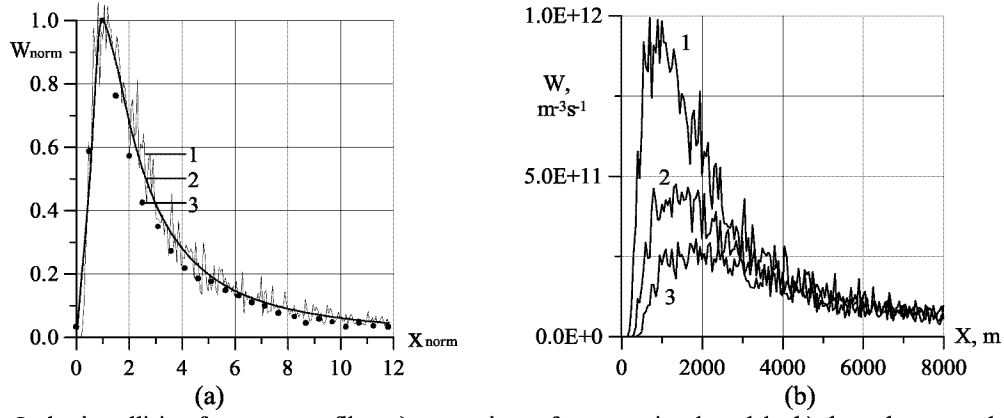


FIGURE 2. Inelastic collision frequency profiles: a) comparison of computational models, b) dependence on elastic collision cross-section.

with complete DSMC result [6] (points 3). The normalized form  $W_{norm} = W / W_{max}$  and  $x_{norm} = x / x_{max}$  is chosen for comparison in accordance with Eq.(6) since it should not depend on uncertainties in choice of values  $\sigma_e, \sigma_{r,eff}$ . The good agreement of the profiles testifies that the adopted simplifications of model are justified.

### 3.2. Analysis.

#### 3.2.2. Dependence on cross-section.

The analytical model not only correctly determines the form of the profile, but also predicts dependencies of the values  $W_{max}$  and  $x_{max}$  from the value of elastic collision cross-section. In a Fig. 2b the profiles of  $W$  on an axis of plume presented for axially symmetric flow for three values of collision cross-section  $\sigma_e = \sigma_{e0} \cdot 10^{-20} m^2$ ,  $1 - \sigma_{e0} = 10$ ,  $2 - \sigma_{e0} = 15$ ,  $3 - \sigma_{e0} = 20$ , and inelastic cross-section  $\sigma_{r1}$  (see 2.2.3.). It is easy to test, that the detected earlier approximate dependencies for a position of maximum  $x_{max}$  and its value  $W_{max}$  from value of  $\sigma_e$  are fulfilled.

In Fig. 3a the profiles of radiance on an axis of a plume are shown at an observation from the side perpendicularly axes of plume,  $W_z(x, y=0) = (h\nu / 4\pi) \int W dz$ , for the same three values of elastic collision cross-section. From this data it follows, that the effective value of elastic collision cross-section between atmospheric oxygen atoms and plume molecules may be detected by results of glow observation from the side provided that the inelastic processes do not influence the form of measured profiles. The absence of such influence is illustrated in

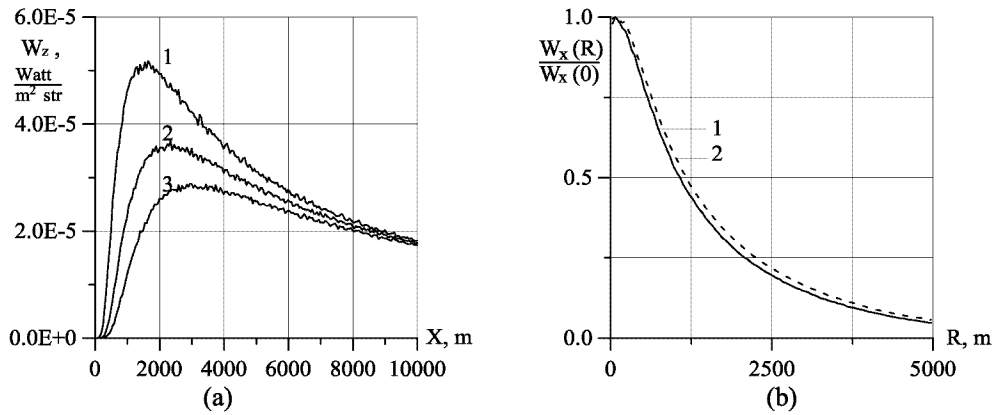


FIGURE 3. Radiance profiles: a) side view  $W_z(x,y=0)$  - dependence on elastic collision cross-section, b) tail view  $W_x(R)$  - dependence on inelastic collision cross-section.

Fig. 3b: the relative profiles of the value  $W_x(R)$  ( $R$ -distance from axis) for two cross-section of the inelastic process, see Eq. (5), are shown at  $\sigma_e = 15 \cdot 10^{-20} \text{ m}^2$ . Difference in the profiles is insignificant. These data justify the splitting processes on two, carried out by analytical model (scattering of fast atmospheric oxygen atoms and inelastic collisions of atoms with molecules of water) not only on an axis of plume.

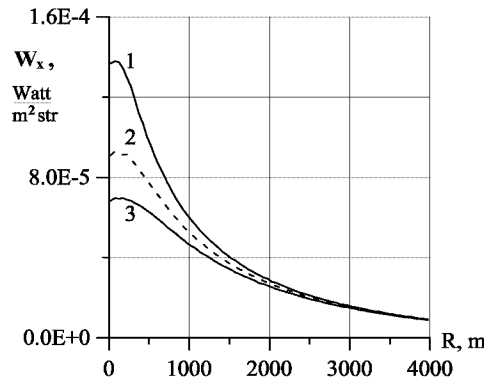


FIGURE 4. Dependence of  $W_x$  on elastic collision cross-section.

In Fig. 4 the profiles of the value  $W_x$ , i.e. dependence of this value on distance from an axis, are shown at the same three values of elastic cross-section. The values of collision cross-section influence the profile of this value, but only at small distance from an axis. At increase of distance this influence disappears. Such dependence is explained by the fact, that outside of plume core the flux of oxygen atoms does not damp.

### 3.2.3. Comparison with experiment.

These results give the possibility to define the value of effective collision cross-section  $\sigma_e$  not only by the measurements of  $W_z$  but also by the measurements transverse profiles, the value  $W_x$ . The result of such determination of the  $\sigma_e$  value is shown in Fig. 5. The normalized profiles  $W_{L,norm}$  observed from the finite distance (see Fig. 1) were used for this purpose, because it does not depend on  $\sigma_r$ . The angle  $\chi$  is the angle between observation line and MIR-SOYUZ line. Curves 1 and 2 correspond to the computation with  $\sigma_e = 7.5 \cdot 10^{-20} \text{ m}^2$  and  $\sigma_e = 15 \cdot 10^{-20} \text{ m}^2$ . Profile derived from the experiment is also shown in the figure. The experimental data are evidently closer to curve 1, that confirms  $\sigma_e$  estimate obtained from beam scattering measurement data (see 2.2.3.) At this computation observation geometry of real experiment performed on 28 February 1999 was used and non-symmetry of the flow was taken into account as well.

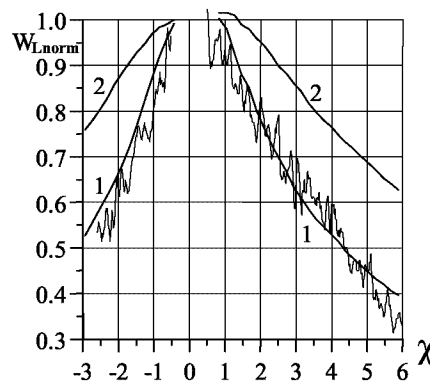


FIGURE 5. Comparison of experimental and numerical normalized radiance profiles.

Figure 6 gives an example of numerical modeling of radiation map observed in the same experiment. This modeling revealed that maximal brightness in the map changed not very much while the observation condition and the flowfield parameters were varied. Assuming the atmosphere parameters and the measured radiation spectral content are known, one could derive the  $\sigma_{r,eff}$  value from these maps. The first result of so comparing of experimental and numerical data leads to the upper limit of effective inelastic collision cross-section  $\sigma_{r,eff} = 0.9 \cdot 10^{-22} m^2$ . This value close to the water photo-dissociation cross-section with  $OH(A)$  coming out as product. The received value  $\sigma_{r,eff}$  is lower than the values, computed by Eq.(5), by factor of 10-25.

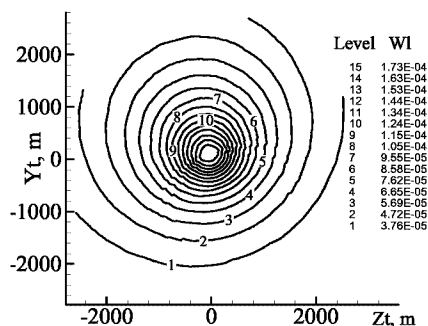


FIGURE 6. Radiation map.

These examples shows that suggested method can be effectively used for analysis of the flowfield and derivation of the cross-section values from the experimental data. It should be noted that accuracy of these derivation may be affected by not only the experimental errors, but by adequacy of the model approximation as well. For instance,  $\sigma_{r,eff}$  derived from the experimental data evidently depends on the degree of water condensation in the rarefied plume. This fact was ignored in the frame of the model. In future we hope to improve physical model of the phenomena and obtain more accurate estimate of the  $\sigma_{r,eff}$  value. And finally – the method suggested here may be used for derivation of the energy dependence of  $\sigma_r(E)$  by solution of inverse problem (see 2.2.4.). This solution will require incorporation of various  $\sigma_{r,eff}$  measured at different angles between the plume axis and atomic oxygen flux velocity.

## REFERENCES

1. Karabadzhak, G. F., Plastinin Yu., et al. "Experimentation Using the Mir Station as a Space Laboratory," *36th AIAA Aerospace Sciences Meeting*, AIAA Paper 98-0288, Reno, NV, January 1998.
2. Karabadzhak, G. F., Plastinin Yu., et al. "Measurements of the Progress-M Main Engine Retrofiring Plume at Orbital Conditions," *37th AIAA Aerospace Sciences Meeting*, AIAA Paper 99-1042, Reno, NV, January 1999.
3. Karabadzhak, G. F., Plastinin Yu., et al., "Mir Based Measurements of the Ultraviolet Emissions from Rocket Exhaust Plume Interactions with the Atmosphere at 380-km Altitude," *38th AIAA Aerospace Sciences Meeting & Exhibit*, AIAA Paper 2000-0105, Reno NV, January 2000.
4. Karabadzhak, G. F., Plastinin Yu., et al. "Preliminary Analysis of Exhaust Plume Radiation during Soyuz-TM Retrofirings", *34th AIAA Thermophysics Conf.*, AIAA-paper 2000-2373, Denver, CO, 2000.
5. Drakes, J. A., Swann, D. G., et al. "Computations of the Progress-M Spacecraft Retrofiring Exhaust Plume," *37th AIAA Aerospace Sciences Meeting*, AIAA Paper 99-0945, Reno, NV, January 1999.
6. Gimelshein, S. F., Levin, D. A., et al., "Modeling of UV Radiation from High Altitude Plumes and Comparison with Data from the Mir Space Station", *33rd AIAA Thermophysics Conference*, AIAA Paper 99-3452, Norfolk, VA, June 1999.
7. Levin, D. A. and Gimelshein, S. F., et al. "Modeling of Emissions from the Soyuz, Progress, and the Mir Rocket Exhaust Plumes at High Altitudes," *38th Aerospace Sciences Meeting*, AIAA Paper AIAA-2000-0601, Reno NV, January
8. Gordeev, O.A., Kalinin, A.P., et al., Reviews on thermophysics, Inst. High Temperature AN USSR, N.5(55), 99p., 1985.
9. Sveta, R.A., Estimated viscosities and thermal conductivities of gases at high temperature, NASA TR, R-132, 1962.
10. Cubley, S.J., Mason, E.A., *Phys. Fluids*, **18**, N.9, 1109-1111, 1975.
11. Bird, G.A., *Molecular Gas Dynamics*, Clarendon Press, Oxford, 1976, Ch. 12.